Electronic Supplementary Material (ESI) for Nanoscale.
This journal is © The Royal Society of Chemistry 2020

Supplemental Material

Doping controlled Fano resonance in bilayer 1T′-ReS_2: Raman experiments and first-principles theoretical analysis

Subhadip Das[1], Suchitra Prasad[2], Biswanath Chakraborty[1,3], Bhakti Jariwala[4], Sai Shradha[4], D. V. S. Muthu[1], Arnab Bhattacharya[4], U. V. Waghmare[2] and A. K. Sood[1*]

[1]*Department of Physics, Indian Institute of Science, Bangalore 560012, India*

[2] *Theoretical Sciences Unit, Jawaharlal Nehru Centre for Advanced Scientific Research, Bangalore 560064, India*

[3] *Present address: Department of Physics, Indian Institute of Technology Jammu, Jammu-181221,J&K, India*

[4]*Department of Condensed Matter Physics and Materials Science, Tata Institute of Fundamental Research, Mumbai 400005, India.*

[*] asood@iisc.ac.in

I. Polar plots of the out-of-plane Raman modes

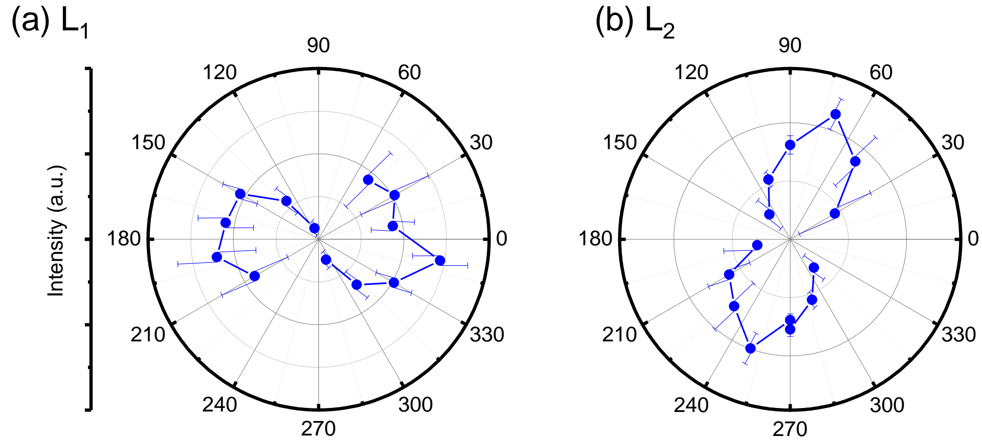

Fig. S1: (a) Raman intensity variation of the A_g-like (a) L_1 and (b) L_2 modes with laser polarization angle θ in unpolarized collection configuration. Intensities of the peaks have been normalized using angular dependence of Si peak at $\sim$520.5 cm^{-1}.

II. Additional tranport data and EPC analysis of 143 cm^{-1} mode of bilayer ReS_2

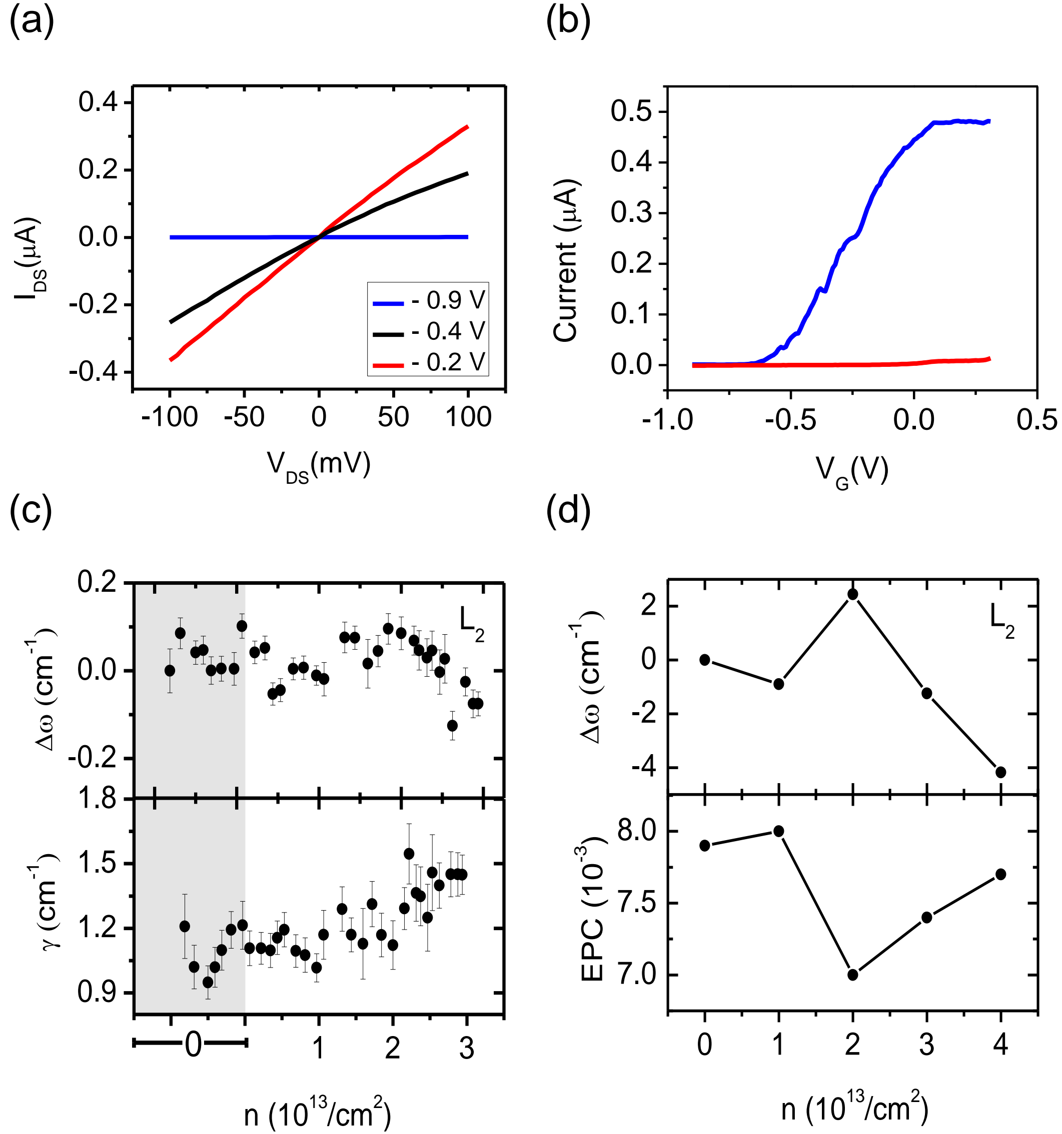

Fig. S2: (a) Drain current (I_{DS}) versus drain voltage (V_{DS}) at three different gate voltages. (b) Negligible gate to source current (red line) compared to the drain to source (blue line) current at 0.1V of drain to source voltage, confirming the absence of Faradaic current in our device transport measurements from Figs. 1(d) and (e) of the main text. (c) Experimental measurements of the frequency shift ($\Delta\omega = \omega(n \neq 0) - \omega(n = 0)$) and linewidth ($\gamma$) with electron doping (n) of the L_2 mode at $\theta = 90^o$. Gray region represents the transistor off-state ($V_G \leq V_{Th}$). (d) Calculated values of $\Delta\omega$ and EPC for the L_2 mode with n.

III. Behavior of the in-plane modes at $\theta = 90^o$

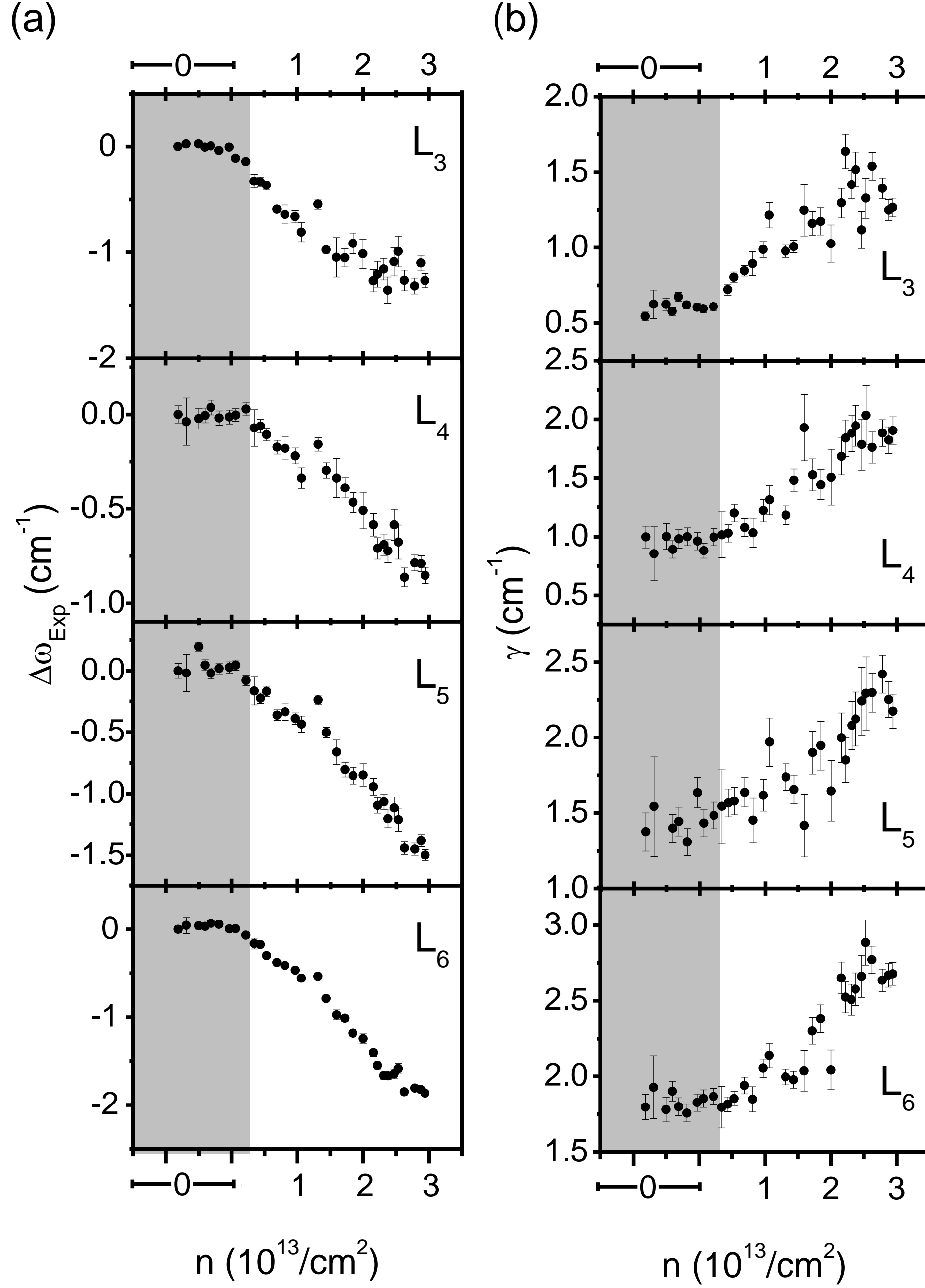

Fig. S3: (a) $\Delta\omega$ and γ versus n at $\theta = 90^o$ for the E_g-like modes.

IV. EPC measurement of trilayer $ReSe_2$

Using similar methods for experimental measurements and theoretical calculations used for bilayer ReS_2 (described in the main text), we have repeated our work on a trilayer $ReSe_2$ transistor. $ReSe_2$ is isostructural to ReS_2 [1, 2], hence there are 18 Raman active mode with A_g symmetry [3]. Unlike ReS_2, the Raman modes of $ReSe_2$ has not been yet classified as in-plane or out-of-plane modes. Atomic force microscopic measurement (inset of Fig. S4(a)) reveals $\sim$ 2.3 nm (3 layers) of sample thickness. Raman spectrum for trilayer $ReSe_2$ (Fig. S4(a)) shows 14 modes, which are labeled from N_1 to N_{14}. The drain current (I_{DS}) with gate voltage (V_G) measurement (Fig. 4(b)) shows electron field-effect mobility of ~ 0.41 cm^2/V.s and current on-off ratio of $\sim 10^2$. Although these parameters are consistent with previous reports [4, 5], the n-type semiconducting behavior can be attributed to unintentional doping during growth process [4]. The Raman modes of trilayer $ReSe_2$ (Fig. S4(a)) at different gate voltages are fitted with a sum of Lorentzian functions to extract the phonon frequency (ω) and linewidth (γ). All 14 modes show small changes in phonon frequency, with maximum phonon softening of ~ 0.6 cm^{-1} observed for N_7, N_{11} and N_{12} modes at n $\sim 5\times10^{13}$/cm^2 (Figs. S5(a, b)). Similarly, the linewidth of all the modes (Figs. S6(a, b)) show little to no change with doping.

We find an indirect band gap of 0.93 eV and 1.02 eV of bulk $ReSe_2$ based on the calculation with and without the inclusion of spin-orbit coupling (SOC). Our results are in good agreement with the earlier theoretical and experimental findings of band gaps of bulk $ReSe_2$ [3, 6]. In trilayer $ReSe_2$, we have tried three different ABA stacking configurations. We displaced the middle layer of $ReSe_2$ by three different distances (d) and obtained the relative energy after z-direction relaxation. We find that the AAA stacking is the most stable of all (Table-S1). For trilayer $ReSe_2$, we see an indirect band gap of 1.12 eV and VBM is a bit away from Γ-point (Fig. S7(a)). After including the SOC in our calculations, we get an indirect band gap of 1.03 eV, with the VBM at Γ-point (Fig. S7(b)). We determined the electronic structure of trilayer $ReSe_2$ in the ABA stacking configuration (stacking 2), which has lower energy than the other ABA stacking configuration. We find an indirect band gap of

1.13 eV for ABA stacking of trilayer $ReSe_2$ (Fig. S7(c)). Also, the electronic structure does not change much with the stacking sequence. Since, AAA stacking (stacking 0) is the most stable of all, we used it in finding the effects of electron doping. We see negligible softening of phonon modes with electron doping (Figs. S5(c, d)). In addition, all the phonon modes show relatively weak coupling with electrons (Figs. S6(c, d)).

The direct band gaps of ReS_2 and $ReSe_2$ at Γ-point are 1.32 eV and 1.22 eV respectively (Figs. 5(a) and S7(a)). In contrast to ReS_2, $ReSe_2$ exhibits an indirect band gap of 1.12 eV (Fig. S7(a)). The VBM of ReS_2 has the highest density of states at Γ-point while, it is slightly offset from Γ in $ReSe_2$. Phonon frequencies are derived from the interatomic force constants which are linear response functions having a dominant contribution from the phonon mediated coupling between electronic states at CBM and VBM. Upon electron doping, the valley of CBM at K-point of $ReSe_2$ gets populated, while that at Γ-point gets populated in ReS_2. As a result, the frontier states at Γ-point are masked from contributing to phonon frequencies in ReS_2 resulting in changes in dominant terms in the interatomic force constant. Hence upon electron doping, a significant change in phonon frequencies of ReS_2 are observed, while little changes are seen in $ReSe_2$ (Fig. S8).

TABLE S1: Energies of stacking configurations (n), (E_n-E_0, N=1,2) and relative displacements (d) between the middle layer of $ReSe_2$ with respect to bottom layer of trilayer $ReSe_2$.

Stackings	Energy (eV)	d (Å)
0	0	(-0.67, -2.19, 6.35)
1	0.34	(-1.48, -0.77, 6.35)
2	0.02	(-2.30, 0.65, 6.35)

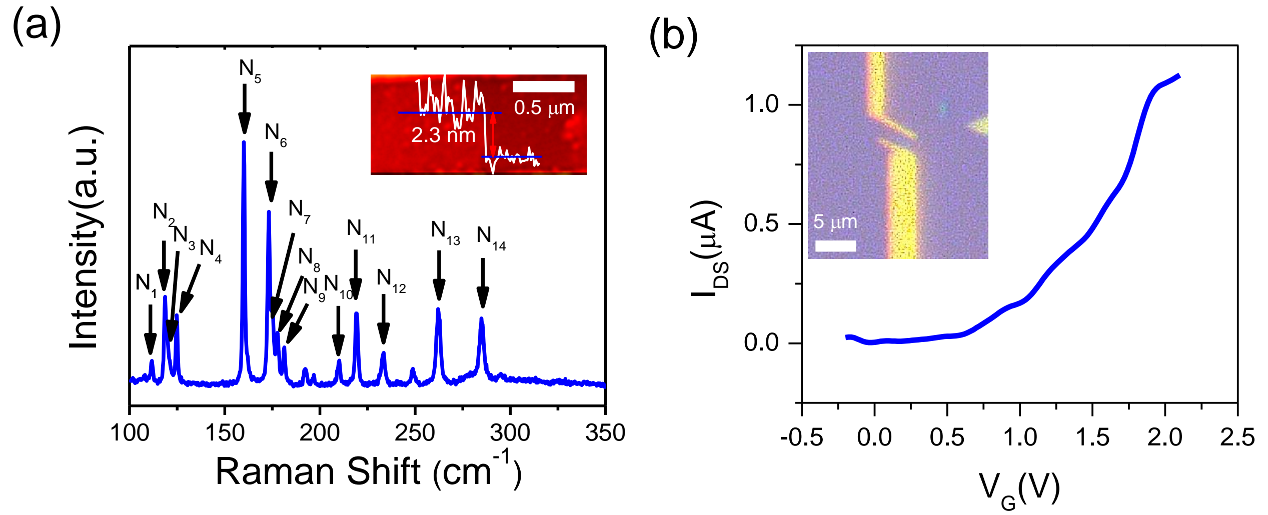

Fig. S4: (a) Raman spectrum of trilayer $ReSe_2$. The modes are indicated as N_1 to N_{14}. Inset image shows the AFM height profile. (b) Drain current (I_{Ds}) as a function of the gate voltage (V_G) with drain voltage fixed at 0.4V. Inset shows the optical image of the device.

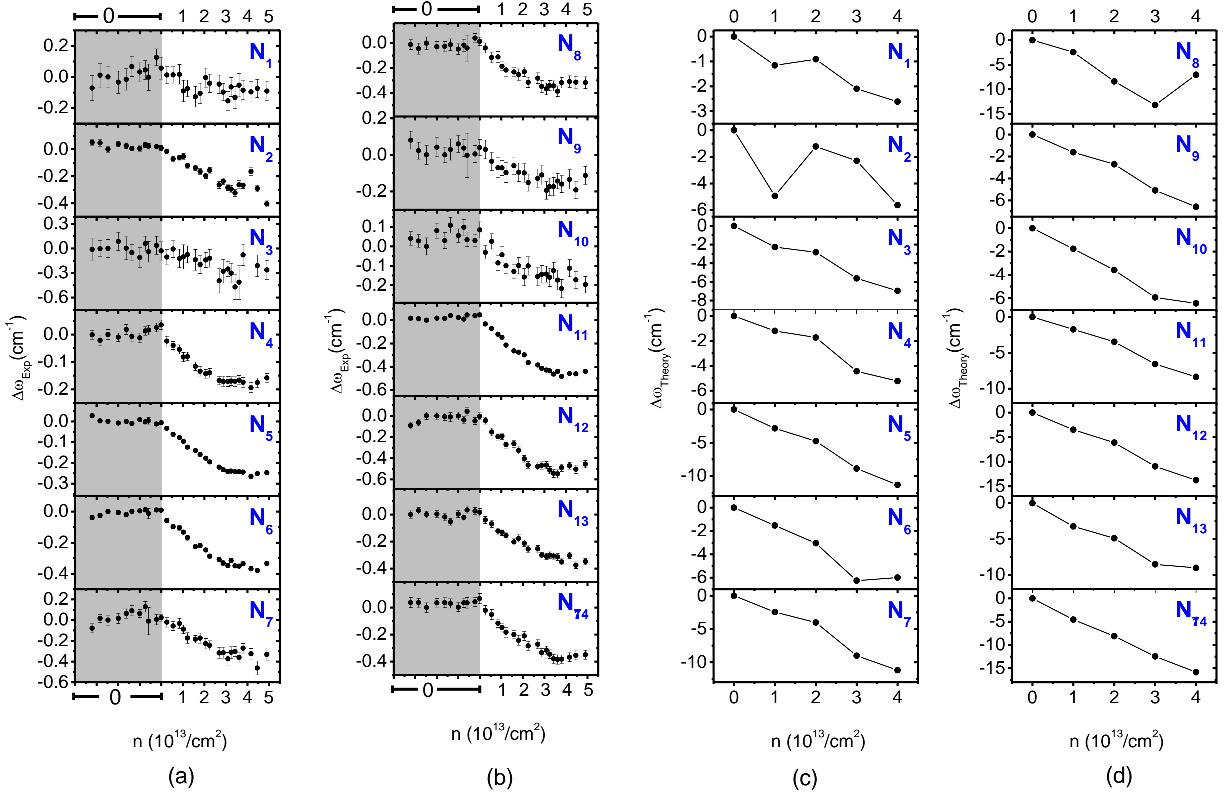

Fig. S5: $\Delta\omega$ versus n from experimental measurements (a, b) and theoretical calculations (c, d) in trilayer $ReSe_2$. Gray region indicates undoped regime.

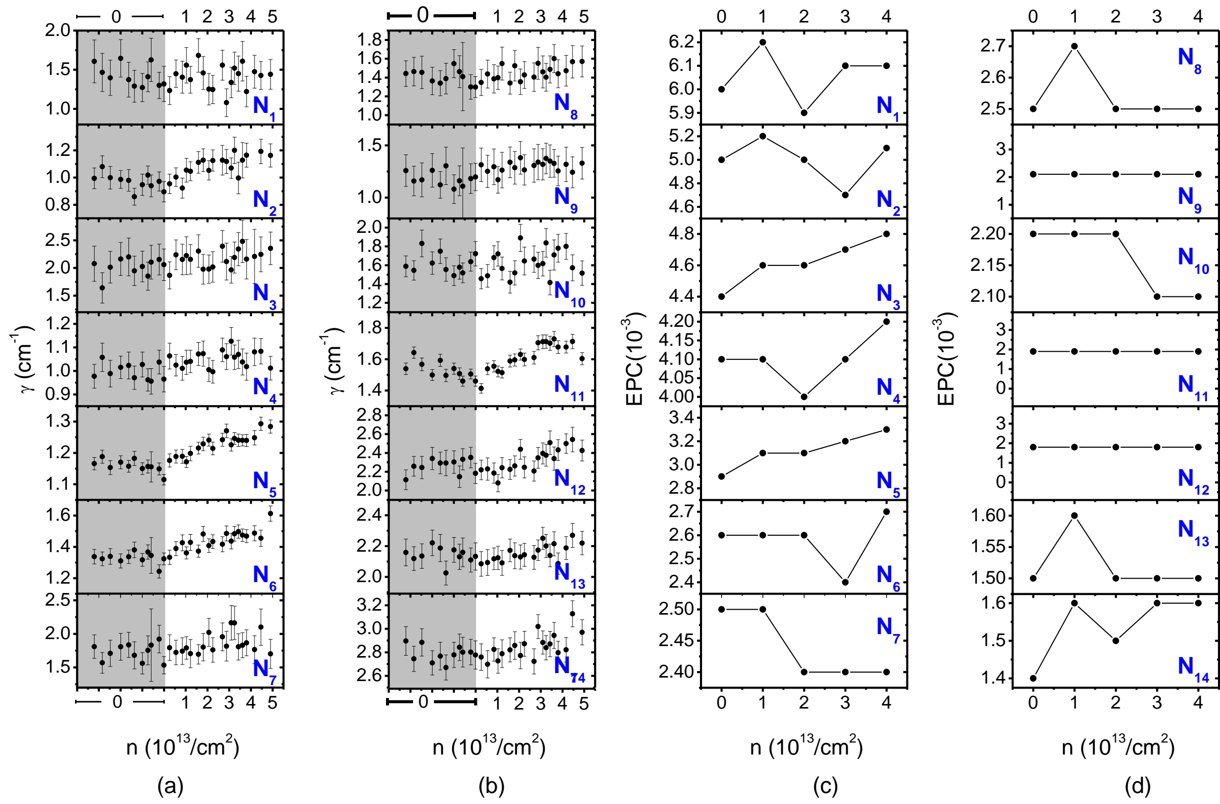

Fig. S6: Experimentally measured γ (a, b) and calculated EPC (c, d) versus n. Gray region represents undoped regime.

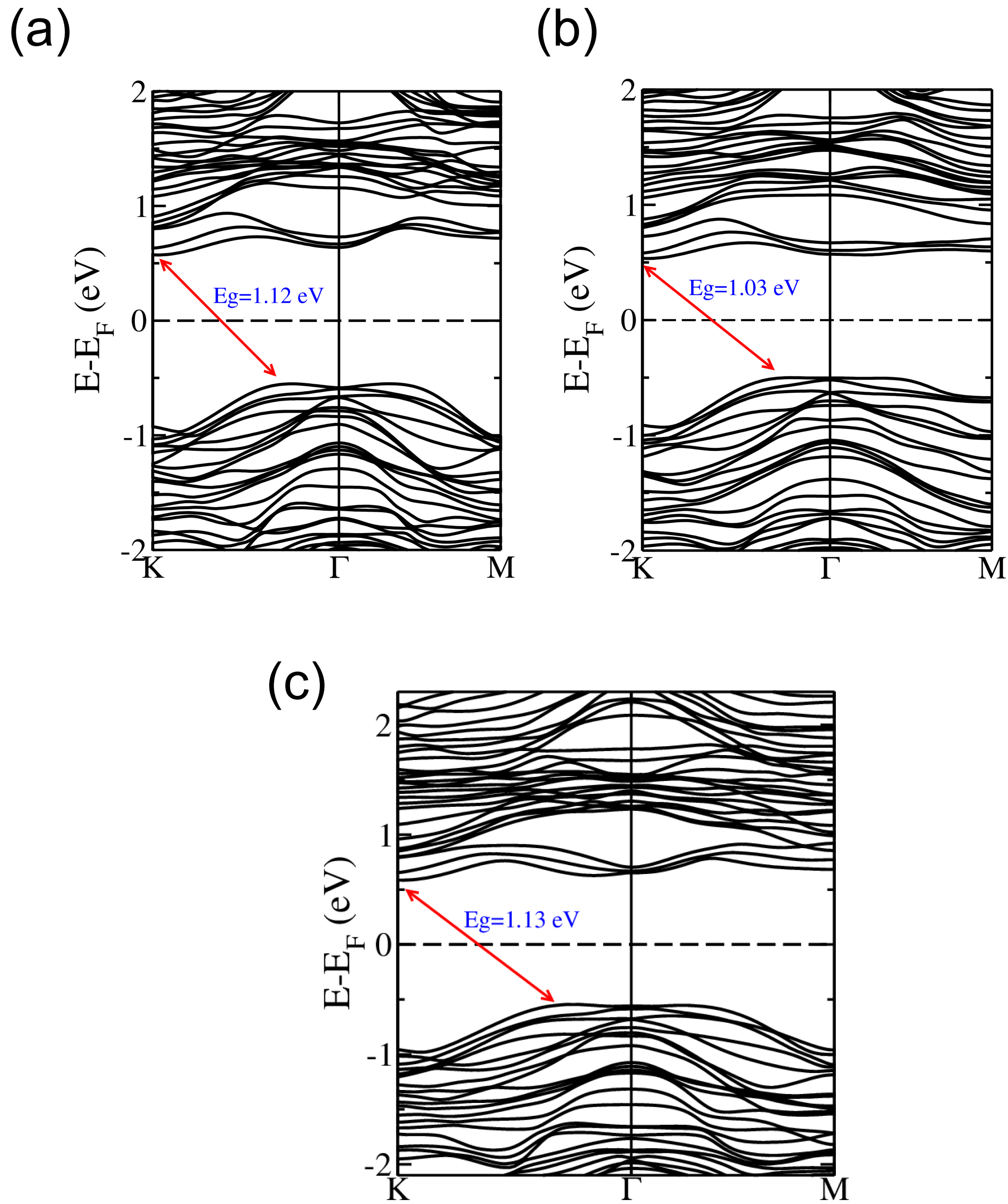

Fig. S7: Electronic structures of trilayer $ReSe_2$ in stacking configuration 0 obtained with (a) SOC = 0, (b) SOC ≠ 0. (c) Electronic structure of trilayer $ReSe_2$ with stacking 2 obtained with SOC=0.

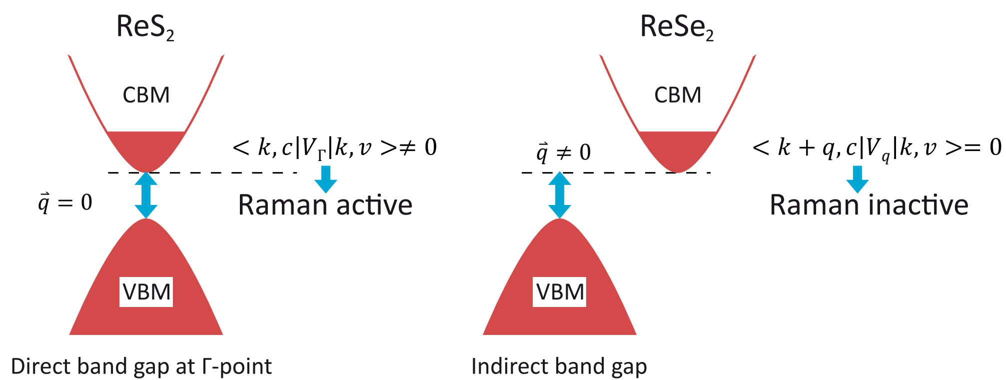

Fig. S8: Schematic illustration of the coupling of electrons with phonons in ReS_2 and $ReSe_2$.

V. Raman spectra at two different spots

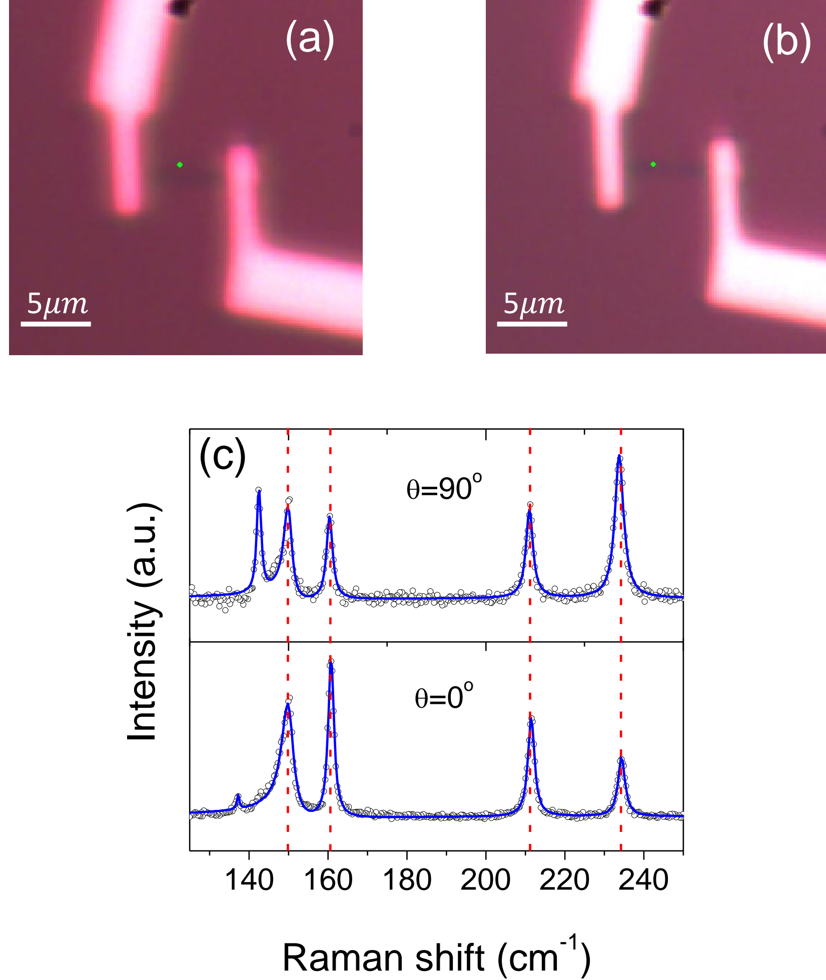

Fig. S9: Different incident laser positions shown by a green dot in the device optical images during (a) doping and (b) dedoping cycle. (c) Raman spectra with the same peak positions taken on these two spots at $n \sim 3 \times 10^{13}/cm^2$ during doping and dedoping cycles at $\theta = 90^o$ and 0°, respectively. Black circles and blue lines are the experimental data points and their cumulative peak fits respectively. As evident from the figure, only the mode at $\sim$ 153 cm^{-1} (labeled L_3 in Fig. 1(c)) shows asymmetric broadening in the low frequency side with the Fano parameter (1/q) of $\sim$ -0.15, whereas other modes show symmetric Lorentzian lineshape. Red dashed lines are guide to the eye for Raman peak position for the in-plane modes.

VI. Bulk band structure calculation of ReS_2

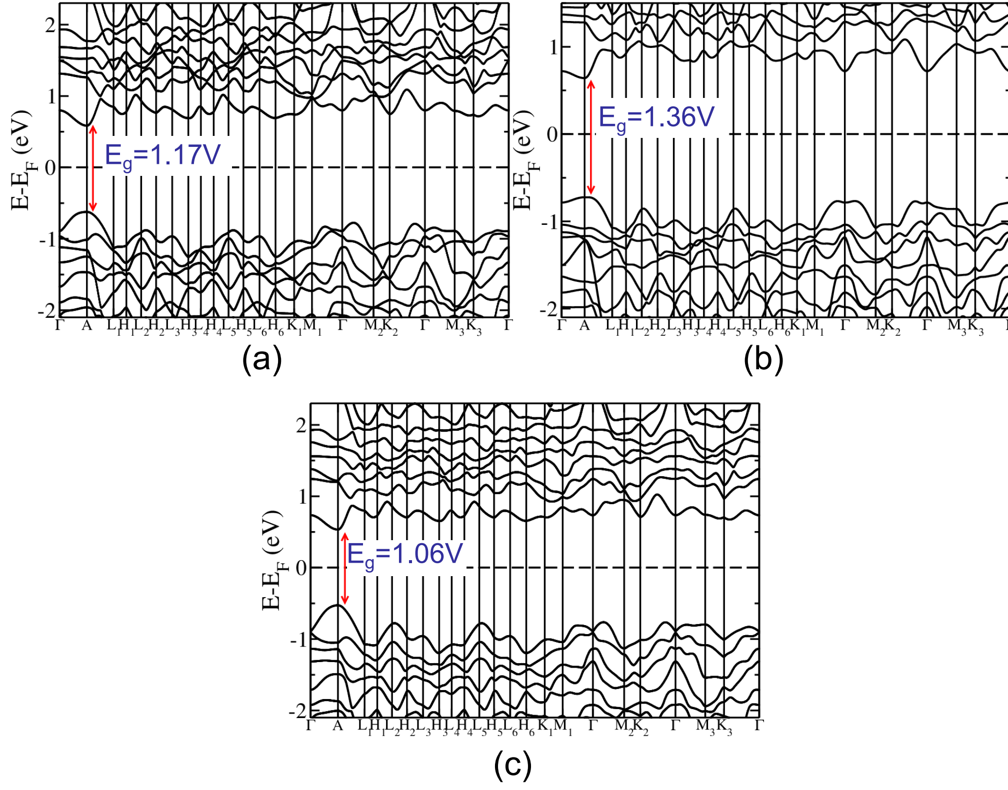

Fig. S10: Electronic band structure of bulk ReS_2 obtained using (a) LDA-USPP, (b) GGA-USPP and (c) LDA-USPP with SOC inclusion.

VII. EPC calculation in stacking 3

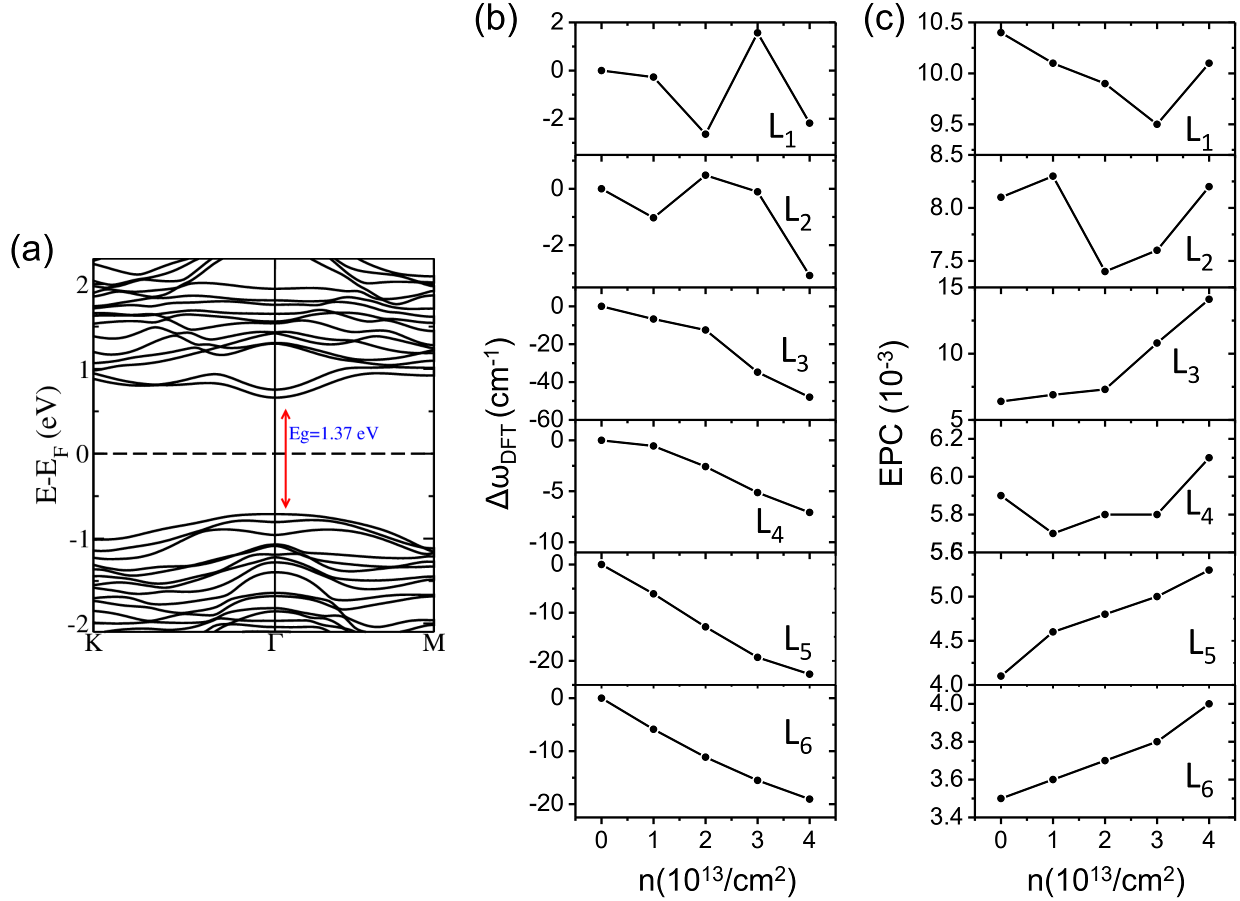

Fig. S11: (a) Electronic band structures of bilayer ReS_2 with stacking 3. (b) Variation in phonon frequencies and (c) electron-phonon coupling with electron doping concentration in bilayer ReS_2 (stacking 3), obtained from first-principles DFT calculations.

---

[1] H.-J. Lamfers, A. Meetsma, G. Wiegers, and J. De Boer, Journal of alloys and compounds **241**, 34 (1996).

[2] J. Wildervanck and F. Jellinek, Journal of the Less Common Metals **24**, 73 (1971).

[3] D. Wolverson, S. Crampin, A. S. Kazemi, A. Ilie, and S. J. Bending, ACS Nano **8**, 11154 (2014).

[4] B. Jariwala, D. Voiry, A. Jindal, B. A. Chalke, R. Bapat, A. Thamizhavel, M. Chhowalla, M. Deshmukh, and A. Bhattacharya, Chemistry of Materials **28**, 3352 (2016).

[5] S. Yang, S. Tongay, Y. Li, Q. Yue, J.-B. Xia, S.-S. Li, J. Li, and S.-H. Wei, Nanoscale **6**, 7226 (2014).

[6] H. Zhao, J. Wu, H. Zhong, Q. Guo, X. Wang, F. Xia, L. Yang, P. Tan, and H. Wang, Nano Research **8**, 3651 (2015).